

Air-core fiber distribution of hybrid vector vortex-polarization entangled states

Daniele Cozzolino¹, Emanuele Polino², Mauro Valeri², Gonzalo Carvacho², Davide Bacco¹, Nicolò Spagnolo², Leif Katsuo Oxenløwe¹, Fabio Sciarrino^{2,*}

¹ *CoE SPOC, Dep. Photonics Eng., Technical University of Denmark, Kgs. Lyngby 2800, Denmark*

² *Dipartimento di Fisica, Sapienza Università di Roma, Piazzale Aldo Moro 5, I-00185 Roma, Italy*

*Email: *fabio.sciarrino@uniroma1.it*

Dated: March 11, 2019

Abstract

Entanglement distribution between distant parties is one of the most important and challenging tasks in quantum communication. Distribution of photonic entangled states using optical fiber links is a fundamental building block towards quantum networks. Among the different degrees of freedom, orbital angular momentum (OAM) is one of the most promising due to its natural capability to encode high dimensional quantum states. In this article, we experimentally demonstrate fiber distribution of hybrid polarization-vector vortex entangled photon pairs. To this end, we exploit a recently developed air-core fiber which supports OAM modes. High fidelity distribution of the entangled states is demonstrated by performing quantum state tomography in the polarization-OAM Hilbert space after fiber propagation, and by violations of Bell inequalities and multipartite entanglement tests. The present results open new scenarios for quantum applications where correlated complex states can be transmitted by exploiting the vectorial nature of light.

Introduction

Quantum communication requires the reliable transmission of quantized information carriers (qubits) among several and spatially separated parties [1], towards development of quantum networks. In particular, protocols based on genuine quantum schemes like entanglement swapping [2–5], superdense coding [6–9] and quantum teleportation [10–16], have to be adopted in future networks to access communication advantages that would be unattainable by using any classical resource. The key element of these schemes is entanglement, which is one of the most distinctive quantum phenomena, predicted by Einstein, Podolsky and Rosen [17], that defies the classical notion of local causality [18]. Quantum correlations are an essential ingredient for quantum foundations studies and for different quantum information processes [19–22]. Great interests has been devoted to the coherent distribution through optical fibers of such quantum correlations, since it constitutes the cornerstone for the future quantum networks [23–26]. Several photon degrees of freedom can be employed for this task, such as frequency, orbital angular momentum (OAM), time and polarization [25–29]. In particular OAM of light is one of the most promising, albeit challenging to manipulate. Photons owning a non-zero OAM are characterized by the azimuthal phase dependence $e^{i\ell\phi}$, where

$\ell\hbar$ is the amount of OAM carried by each photon, and ℓ is an unbounded integer value representing discrete quantum states [30, 31]. Due to its unbounded nature, OAM has been largely investigated both for classical and quantum communications, being capable of encoding high dimensional quantum states (qudits), which enhance the photon information capacity [32–43]. Experimental investigations on OAM supporting fibers for classical communications have been reported [32, 33, 44–46]. Still, distribution of quantum states through multimode fibers supporting OAM modes is a newborn research field, where only few experiments have been realized to date [47, 48]. In reference [47], high-dimensional quantum states, encoded in weak coherent pulses, have been transmitted and detected through a 1.2 km length air-core fiber at telecom wavelength, demonstrating the feasibility of high-dimensional quantum communication and quantum key distribution protocols. In reference [48], a solid core vortex fiber has been exploited, demonstrating the possibility of two-dimensional quantum communication with structured photons. Nonetheless, experiments investigating the transmission of entangled photon pairs still need to be explored.

In this work, we demonstrate distribution of hybrid entanglement between a linearly polarized photon and a vector vortex (VV) beam, *i.e.* a doughnut-shaped

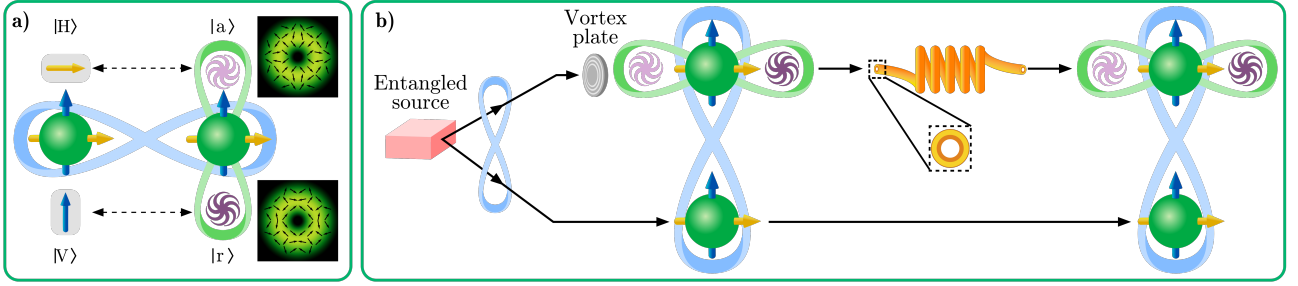


Figure 1: **Hybrid entangled state transmission.** **a)** Hybrid VV-polarization entangled photon pair generated in the experiment: entanglement in polarization of the photon pair (blue ribbon) and entanglement between polarization and OAM of the single photon (green ribbon, VV state) are sketched. The inhomogeneous polarization patterns of the VV state $|r\rangle$ (bottom) and $|a\rangle$ (up) are explicitly shown. **b)** Schematic of the experiment: hybrid VV-polarization entangled state is generated by an initial polarization entangled photon pair. One photon of the pair encodes the VV state by the action of a vortex plate. The VV beam is transmitted through the air-core fiber. Finally, state detection shows that hybrid VV-polarization entanglement (blue and green ribbons) is preserved after fiber transmission.

beam with an inhomogeneous polarization pattern, at telecom wavelength. The VV beam is transmitted through a 5m long air-core fiber [49], whose very low mode mixing preserves OAM states and, in turn, hybrid entanglement. This peculiar feature opens up new scenarios and opportunities in quantum communications towards fiber based quantum networks, enabling the capability to employ high dimensional quantum states, embedded in the photon polarization and OAM degrees of freedom.

Vector vortex beam and hybrid entanglement generation

Vector vortex beams constitute a special class of vector beams, which are characterized by an inhomogeneous polarization distribution over their transverse profile [50]. In particular, a VV beam has an azimuthally varying polarization pattern, surrounding a central optical singularity [51–53]. Due to their distinctive polarization distributions, VV beams have shown unique features, making them appealing for different research purposes, *e.g.* microscopy [54], optical trapping [55,56], metrology [57,58], nanophotonics [59] and communication [60–67]. Formally, the state $|R, \ell\rangle$ ($|L, \ell\rangle$) describes a photon with uniform right (left) circular polarization carrying $\ell\hbar$ of OAM, and a VV beam can be conveniently described by a non-separable superposition of polarization-OAM eigenmodes. In this superposition, OAM quanta carried by the photons define the order m of the VV beam. In particular, a VV beam belongs to a Hilbert space spanned by states $\{|R, m\rangle, |L, -m\rangle\}$ [53]. For instance, if $m = 1$ and if we consider equally distributed superpositions $|r_1\rangle = (|R, +1\rangle + |L, -1\rangle)/\sqrt{2}$ and $|a_1\rangle = (|R, +1\rangle - |L, -1\rangle)/\sqrt{2}$, radially and azimuthally polarized beams are obtained [51,52].

Here we experimentally demonstrate fiber distribution of a VV-polarization entangled photon state. The conceptual scheme of the experiment is reported in Fig. 1. A polarization-VV beam entangled photon pair is gen-

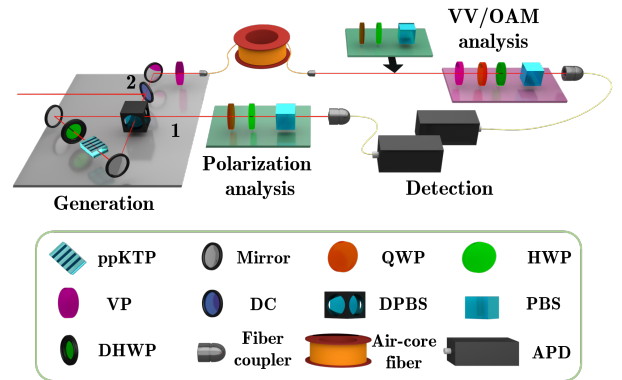
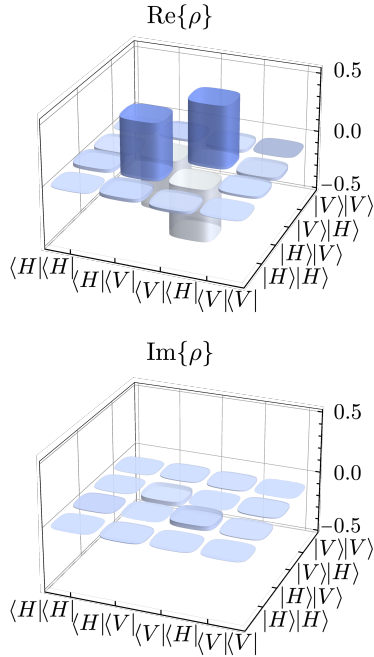


Figure 2: **Experimental apparatus for the generation, distribution and analysis of the hybrid entangled states.** Pairs of telecom polarization entangled photons are generated by exploiting a periodically poled titanyl phosphate crystal (ppKTP) in a Sagnac interferometer, which contains a dual-wavelength polarizing beam splitter (DPBS) and a dual half-wave plate (DHWP). Photons exiting along mode 1 are sent to a polarization analysis stage, composed of a quarter-wave plate (QWP), half-wave plate (HWP) and a polarization beam splitter (PBS). Photons along mode 2 pass through a dichroic mirror (DC), which separates the pump from the photons. Photons in mode 2 impinge on a vortex plate (VP) to generate a VV beam state and, in turn, the desired hybrid entangled state. The VV states are coupled to an air-core fiber and then measured with an OAM-polarization analysis stage composed of a second VP followed by a polarization analysis setup. To perform the measurements on the polarization and OAM degrees of freedom independently, an additional polarization measurement stage has to be inserted before the OAM-to-Gaussian conversion regulated by the second VP. Finally, both photons are coupled into single-mode fibers linked to avalanche photodiode single photon detectors (APDs).

erated from an initial polarization entangled pair (blue ribbon). Only one photon of the pair encodes the VV state (green ribbon). Subsequently, the VV beam is

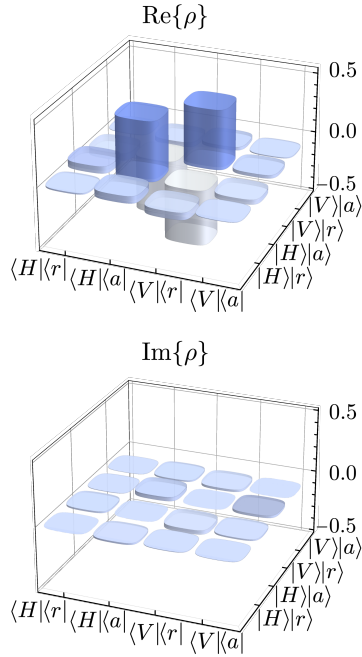
a) Source entanglement

$$|\psi_s\rangle = \frac{1}{\sqrt{2}}(|H\rangle_1 |V\rangle_2 - |V\rangle_1 |H\rangle_2)$$



b) Hybrid entanglement

$$|\psi\rangle = \frac{1}{\sqrt{2}}(|H\rangle_1 |a\rangle_2 - |V\rangle_1 |r\rangle_2)$$



c) Intra-system entanglement

$$|r\rangle = \frac{1}{\sqrt{2}}(|R\rangle | +7\rangle + |L\rangle | -7\rangle)$$

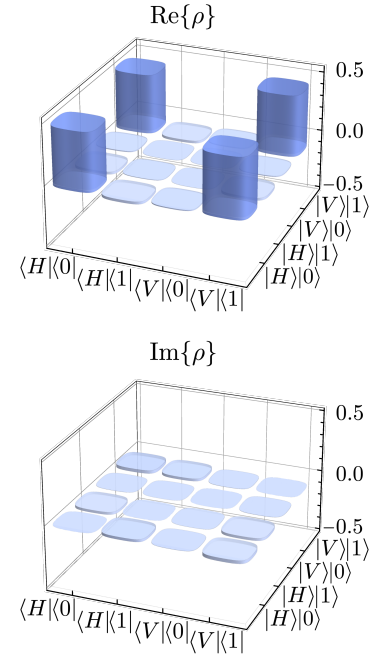


Figure 3: **Two-qubit quantum tomographies.** **a)** Real (top) and imaginary (bottom) parts of the measured density matrix of the polarization entangled state generated by the source, before conversion in OAM. **b)** Real (top) and imaginary (bottom) parts of the measured density matrix of the two-photon VV-polarization entangled state after the transmission of photon 2 through the OAM fiber. **c)** Real (top) and imaginary (bottom) parts of the measured density matrix of the VV state on photon 2, transmitted through the OAM fiber. The OAM states $|0\rangle$ and $|1\rangle$ in the tomography are defined by the relations: $|0\rangle \equiv (|+7\rangle + |-7\rangle)/\sqrt{2}$ and $|1\rangle \equiv i(|-7\rangle - |+7\rangle)/\sqrt{2}$. Real and imaginary parts of the experimental density matrices are reconstructed via quantum state tomographies.

coupled and transmitted through the 5m long air-core fiber and then measured together with the linearly polarized photon. In our case, VV beams of order $m = 7$ are generated, whose expressions are:

$$|r_7\rangle = \frac{|R, +7\rangle + |L, -7\rangle}{\sqrt{2}} \quad (1)$$

$$|a_7\rangle = \frac{|R, +7\rangle - |L, -7\rangle}{\sqrt{2}}. \quad (2)$$

The polarization patterns associated to states $|r_7\rangle$ and $|a_7\rangle$ are shown in Fig. 1a. In the following, we will refer to $|r_7\rangle$ and $|a_7\rangle$ as $|r\rangle$ and $|a\rangle$, respectively. The experimental apparatus is reported in Fig.2. Polarization entangled photon pairs, $(|H\rangle |V\rangle + e^{i\phi} |V\rangle |H\rangle)/\sqrt{2}$, are generated at 1550 nm wavelength by a periodically poled potassium titanyl phosphate (ppKTP) crystal placed into a polarization Sagnac interferometer and pumped with a continuous-wave laser at 775 nm. Indeed, for fiber-based quantum communication, it is important to exploit photons within the C-band (1530-1565 nm), where optical fibers show minimal losses. The relative phase ϕ of the entangled state is controlled to generate the singlet state:

$$|\psi\rangle_s = \frac{1}{\sqrt{2}}(|H\rangle_1 |V\rangle_2 - |V\rangle_1 |H\rangle_2) \quad (3)$$

where the subscripts 1 and 2 indicate the two interferometer output modes. According to the notation in Fig. 2, photons along output mode 2 impinge on a vortex plate (VP), adding OAM order $m = 7$. The VP can be considered as a non-tunable q -plate (QP), *i.e.* a device that couples the polarization and the OAM of a single photon [68]. Specifically, in the circular polarization basis $\{|R\rangle, |L\rangle\}$, the action of a QP with topological charge q , on a single photon of OAM order k , is described by the transformation: $|L, k\rangle \xrightarrow{\text{QP}} |R, k + 2q\rangle$ and $|R, k\rangle \xrightarrow{\text{QP}} |L, k - 2q\rangle$. In our case, $m = 2q = 7$ and the initial OAM order is $k = 0$. Exploiting the spin-orbit coupling, we generate the VV state $|r\rangle$ or $|a\rangle$ depending on the input polarization state, $|H\rangle$ or $|V\rangle$ respectively [69, 70]. Thus, the polarization entangled singlet state is transformed into the hybrid entangled state:

$$|\psi\rangle = \frac{1}{\sqrt{2}}(|H\rangle_1 |a\rangle_2 - |V\rangle_1 |r\rangle_2). \quad (4)$$

The versatility of our experimental approach is based on full control of each degree of freedom through suitable optical components, allowing the preparation of the desired hybrid VV-polarization entangled state (Eq.(4)).

Hybrid entanglement distribution and measurement

The main purpose of our work is to prove the feasibility of entanglement distribution with OAM states transmitted through an air-core fiber. In particular, we demonstrate that the coherence of the complex hybrid entangled state in Eq.(4) is preserved. This is possible since the states $|r\rangle$ and $|a\rangle$ are superposition of anti-aligned states, *i.e.* spin (polarization) and OAM with opposite sign, hence the VV beams are degenerate in time along the fiber transmission [49]. Indeed, an eventual non-degeneracy of those states could impair the coherence of the VV states and, therefore, of the entangled pair. The quality of the transmitted states is measured through tomography processes [71] and their entanglement is certified through CHSH-like inequality violations [72] and tripartite entanglement tests [73–78].

Source state. As a first step, we characterize the initial polarization entangled state in (3). To fully determine the quality of the state generated by the pp-KTP source, we perform a quantum state tomography within the polarization space of the two photons. The measurements are implemented by collecting two-fold detection after two polarization analysis stages placed along each output mode of the source. The obtained tomography is shown in Fig.3a, where the relative fidelity with respect to the ideal singlet state is $F_s = (93.5 \pm 0.2)\%$. Furthermore, we carry out a non-locality test obtaining as the maximum value S of the CHSH inequality $S_s^{(raw)} = 2.67 \pm 0.01$ [72]. Subtracting the accidental coincidences from $S_s^{(raw)}$, such parameter becomes $S_s = 2.68 \pm 0.01$.

Hybrid entangled state (HyEnt). Subsequently, we consider the global hybrid VV-polarization entangled state in (4) and measure the two-fold detection after the VV state propagation through the air-core fiber. The fiber structure allows the transmission of OAM modes with very low mode mixing among them. It is composed by a central air core surrounded by a high refractive index ring, creating a large refractive index step that shapes the field of the modes, allowing for their guidance. The fiber we used supports OAM modes with $\ell = \pm 5, \pm 6, \pm 7$ and has 1 dB/km losses [49]. In our experiment we have decided to work with modes $\ell = \pm 7$, achieving a coupling efficiency $\eta = 0.5$. At this stage, we consider that the entangled two qubit state lies in a 4-dimensional space spanned by the basis $\{|H\rangle_1 |a\rangle_2, |V\rangle_1 |a\rangle_2, |H\rangle_1 |r\rangle_2, |V\rangle_1 |r\rangle_2\}$, that is composed by the polarization of photon 1 and the VV states of photon 2. The qubit encoded in photon 1 is measured by a polarization analysis stage (green platform in Fig.2). Conversely, the measurements of the VV qubit, *i.e.* photon 2, are implemented by a VP, identical to the one used in the generation process, and a polarization analysis stage (purple platform in Fig.2). The VP converts back the VV beam to the

Table 1: **CHSH violations.** The CHSH violation parameters obtained from raw data (S^{raw}) and by subtracting for accidental coincidences (S), are reported for the polarization entangled state generated by the source, the hybrid VV-polarization entangled state (HyEnt) and the intra-system entangled VV state embedded in the photon 2 and transmitted through the air-core fiber (Intra).

State	Measurement Time	$S^{(raw)}$	S
Source	160s	2.67 ± 0.01	2.68 ± 0.01
HyEnt	2560s	2.62 ± 0.03	2.67 ± 0.03
Intra	1920s	2.76 ± 0.05	2.82 ± 0.05

fundamental Gaussian-like mode, restoring the initial polarization state for photon 2 before impinging on the first VP. In this way, the VV states $|r\rangle$ and $|a\rangle$ are directly mapped into polarization states $|H\rangle$ and $|V\rangle$, which are measured with the usual set of quarter-wave plate (QWP), half-wave plate (HWP) and a polarization beam splitter (PBS) (see Fig.2) [61, 69, 70]. State tomography in the 4-dimensional space is reported in Fig.3b. We consider as target state the ideal evolution of the density matrix describing the experimental state generated by the source. The resulting fidelity between such state and the state measured after the fiber propagation is $F_h = (97.9 \pm 0.2)\%$. Furthermore, we observe violation of the CHSH inequality, obtaining the value $S_h^{(raw)} = 2.62 \pm 0.03$ for raw data and value $S_h = 2.67 \pm 0.03$ by subtracting for accidental coincidences, thus violating by 21 and 22 standard deviations the separable limit $S = 2$ respectively.

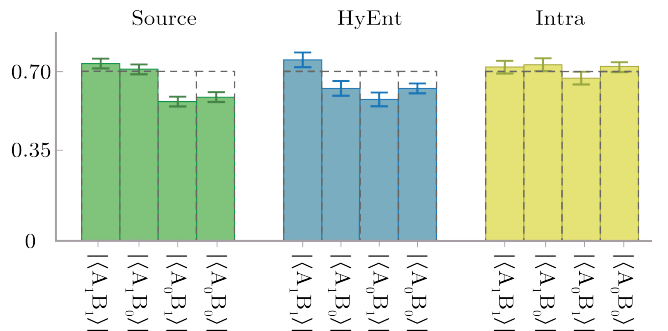


Figure 4: **CHSH measurement operators.** Expectation values moduli of the measured operators that maximize the violation of the CHSH parameter $S = \langle A_1 B_1 \rangle - \langle A_1 B_0 \rangle + \langle A_0 B_1 \rangle + \langle A_0 B_0 \rangle$. The values are relative to the polarization entangled state generated by the source (green bars), the hybrid VV-polarization entangled state (blue bars) and the intra-system entangled VV state embedded in the photon 2 and transmitted through the air-core fiber (yellow bars). All error bars are due to Poissonian statistics of the measured events.

Three qubit state tomography

$$|\psi\rangle = \frac{1}{\sqrt{2}}(|H\rangle_1 |a\rangle_2 - |V\rangle_1 |r\rangle_2) = \frac{1}{\sqrt{2}}(|L\rangle_1 |L\rangle_2 | -7\rangle_2 - |R\rangle_1 |R\rangle_2 | +7\rangle_2)$$

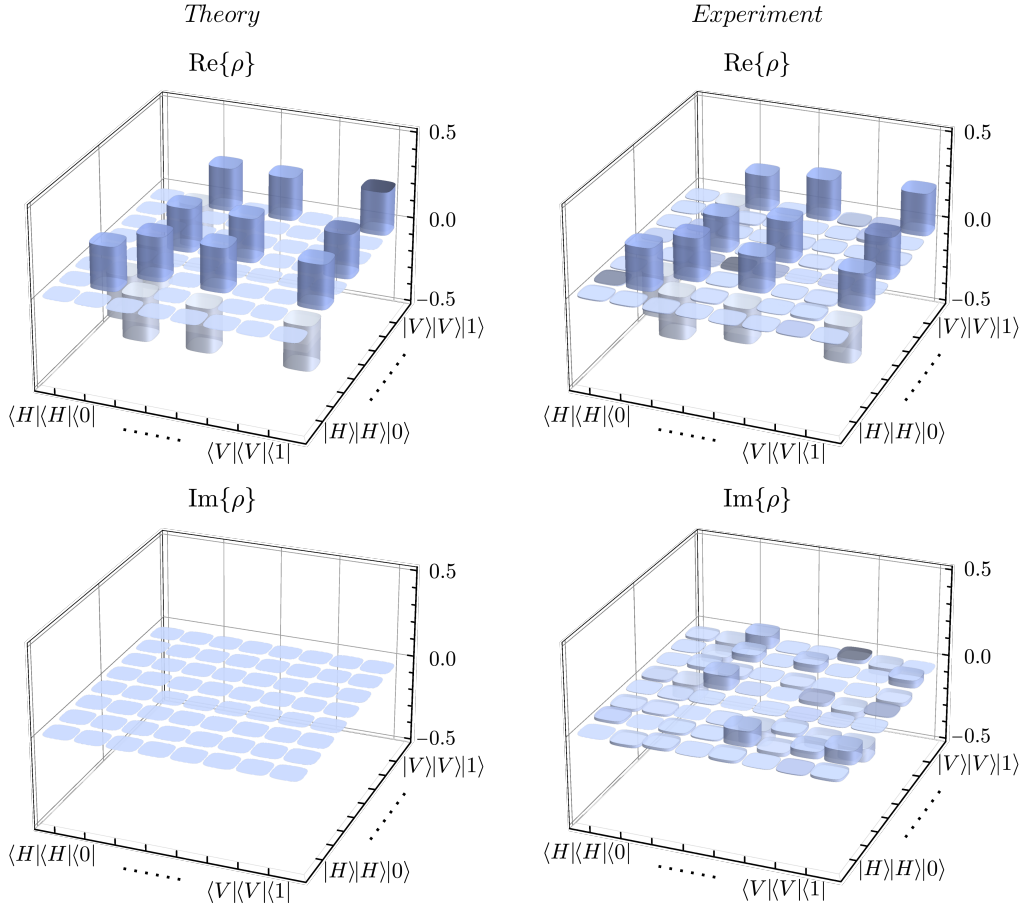


Figure 5: **Three-qubit quantum tomography.** Real and imaginary parts of the measured density matrix of the hybrid VV-polarization state in space $\{|pol\rangle_1 |pol\rangle_2 |oam\rangle_2\}$ after the fiber transmission (right) and of the theoretical density matrix of state in (4) (left). The OAM states $|0\rangle$ and $|1\rangle$ in the tomography are defined by the relations: $|0\rangle \equiv (|+7\rangle + |-7\rangle)/\sqrt{2}$ and $|1\rangle \equiv i(-7) - |+7\rangle/\sqrt{2}$. Real and imaginary parts of the experimental density matrices are reconstructed via quantum state tomography.

Intra-system entangled state (Intra). Now, we focus on the VV state embedded in photon 2 and its transmission through the air-core fiber. Such analysis quantifies the quality of the VV beam state generation, transmission through the air-core fiber and conversion to the fundamental Gaussian mode. The single photon VV states $|r\rangle$ and $|a\rangle$, (1) and (2), are maximally entangled in the OAM and polarization degrees of freedom. They corresponds to single-particle entanglement states, referred to as *intra-system* entanglement. The non-separability between polarization and OAM states is not related to nonlocal properties, since they are relative to the same physical system. However, Bell-like inequalities can be exploited to demonstrate the single-particle entanglement, ruling out models that assume realism and non-contextuality of commuting observables, relative to such systems [79–82]. Hence, we certify the presence of intra-system entanglement carrying out quantum state tomography and performing

CHSH-like inequality in the space of polarization and OAM degrees of freedom of photon 2. Horizontally polarized heralded single photons are sent to the VP to conditionally prepare state state $|r\rangle$ for photon 2. The measurements on the polarization and the OAM degrees of freedom of photon 2 are performed independently. For this purpose, two cascaded measurement stages are needed (green and purple platforms in Fig.2). A first stage (HWP, QWP and PBS) performs the polarization analysis (green platform in Fig.2). The second stage composed of a VP and a polarization analysis (purple platform in Fig.2), measures the photon state in the OAM space. As before, the VP maps the information encoded in OAM to a polarization state, which is then measured. Finally, before detection the photon is coupled to a single mode fiber, tracing out all OAM contributions different from the zero order. The measured quantum state tomography is shown in Fig. 3c and the relative fidelity calculated with re-

spect to the Bell state $|\Phi^+\rangle$ is $F_i = (99.4 \pm 0.6)\%$. The corresponding parameters S_i obtained from the CHSH-like inequality violations are $S_i^{(raw)} = 2.76 \pm 0.05$ and $S_i = 2.82 \pm 0.05$. The set of CHSH violations measured for each state (source, HyEnt and Intra) is summarized in table 1 and the mean values of the measured operators are shown in Fig.4.

Three qubits HyEnt. The previous measurements have independently certified the high fidelity of both the hybrid VV-polarization entangled state and the single photon VV beam state after propagation in the air-core fiber. To complete the characterization of the hybrid VV-polarization entangled state in (4), we now measure such state with a different apparatus that does not assume a 2-dimensional Hilbert space for photon 2 spanned by $\{|r\rangle, |a\rangle\}$. In this case, the state in (4) corresponds to a 3-qubit state that lives in the 2^3 dimensional Hilbert space spanned by the basis of three qubits $\{|pol\rangle_1 |pol\rangle_2 |oam\rangle_2\}$, encoded in the polarizations of the two photons and the OAM degree of freedom of photon 2. The measurements on the final state are performed by a polarization analysis stage for photon 1, and by polarization and OAM analysis stages for photon 2, as the one adopted for the intra-system entanglement characterization (Fig.2). This apparatus allows to measure independently the polarization and the OAM component of photon 2. Thus, performing the 2^3 -dimensional quantum state tomography of the transmitted state (Fig.5), a final fidelity $F = (88.1 \pm 0.2)\%$ with respect to the ideal state in Eq.(4) is obtained, thus showing that the fiber preserves the injected state. As for the other cases, also for the 3-qubit case we perform a device independent test of the quantum correlations, showing their preservation after fiber transmission of the VV state. First, we test the Mermin-Ardehali-Belinskii-Klyshko inequality [73–75], which provides an upper bound for contextual hidden variable theories describing the correlations between observables relative to three qubits:

$$\begin{aligned} \mathcal{M} \equiv & |\langle A_1 B_2 C_2 \rangle + \langle A_2 B_1 C_2 \rangle + \\ & + \langle A_2 B_2 C_1 \rangle - \langle A_1 B_1 C_1 \rangle| \leq 2. \end{aligned} \quad (5)$$

The observables A_i , B_i and C_i ($i = 1, 2$) are dichotomic (with eigenvalues ± 1) and relative to the first, the second and the third qubit, respectively. Violation of such inequality certifies the nonclassical correlations of tripartite states. Furthermore, if a value $\mathcal{M} \geq 2\sqrt{2}$ is found, models in which quantum correlations are allowed between just two of the three qubits (biseparable quantum models), are ruled out as well [83, 84]. The state (4) in the 2^3 -dimensional space is able to reach the algebraic value of $\mathcal{M} = 4$ by choosing the operators: $A_1 = -\sigma_z^A$, $A_2 = \sigma_x^A$, $B_1 = -\sigma_z^B$, $B_2 = \sigma_x^B$, where σ_i ($i = x, z$) are the Pauli operators relative to photons 1 (A) and 2 (B) in the polarization in basis $\{|H\rangle, |V\rangle\}$; and $C_1 = \sigma_z^C$, $C_2 = \sigma_x^C$,

where the Pauli operators are in the OAM basis $\{|0\rangle \equiv (|+7\rangle + |-7\rangle)/\sqrt{2}$, $|1\rangle \equiv i(|-7\rangle - |+7\rangle)/\sqrt{2}\}$ relative to photon 2. Measuring such operators after the VV state transmission and calculating the parameter \mathcal{M} , we obtain $\mathcal{M}^{(raw)} = 3.43 \pm 0.04$ from raw data, and the value $\mathcal{M} = 3.53 \pm 0.04$ by subtracting accidental coincidences. In this way, we violated the classical bound by 35 and 38 standard deviations and the quantum biseparable bound by 15 and 17 standard deviations, respectively.

Finally, we further study the correlation of the state in (4) by performing a Hardy test [76, 77], recently generalized in a suitable form for more than two parties by [78]. Given a system with certain null correlation probabilities, a paradox arises when other events are automatically forbidden in the framework of noncontextual hidden variable models, while they can happen within a quantum context. Since experimentally measuring null probabilities represents a difficult task, Hardy logical contradictions can be conveniently mapped into more general inequalities. In Ref. [78] an extended multi-party version of Hardy's paradox is proposed, leading to an inequality that for three qubits reads:

$$\begin{aligned} \mathcal{H} \equiv & P(A_1 A_2 A_3) - P(A_1 B_2 B_3) - P(A_1 \bar{B}_2 \bar{B}_3) + \\ & - P(B_1 A_2 B_3) - P(\bar{B}_1 A_2 \bar{B}_3) - P(B_1 B_2 A_3) + \\ & - P(\bar{B}_1 \bar{B}_2 A_3) \leq 0, \end{aligned} \quad (6)$$

where A_i (B_i) represents a dichotomic operator A (B) acting on qubit $i = 1, 2, 3$ with eigenvalues ± 1 , $\bar{B}_i \equiv -B_i$ and the probabilities $P(X_1 Y_2 Z_3) \equiv P(X_1 = 1, Y_2 = 1, Z_3 = 1)$. In our case, the transmitted 3-qubit state permits to maximally violate the generalized Hardy test by choosing the operators: $A_1 = A_2 = -A_3 = \sigma_z$ and $B_1 = B_2 = B_3 = \sigma_x$ relative to the qubits $|pol\rangle_1$ and $|pol\rangle_2$ (in basis $\{|H\rangle, |V\rangle\}$) and $|oam\rangle_2$ (in basis $\{|0\rangle, |1\rangle\}$), respectively. The experimental value \mathcal{H} obtained for raw data is $\mathcal{H}^{(raw)} = 0.085 \pm 0.008$ and by accounting for accidental coincidences it becomes $\mathcal{H} = 0.104 \pm 0.008$ (theoretical value for the ideal state is $\mathcal{H} = 0.25$). Such values allow to violate the noncontextual bound by 10 and 12 standard deviations, respectively. Note that, the tripartite correlations obtained are generated by both contextual (intrasystem) and nonlocal (intersystem) entanglement.

Conclusions and discussion

Future quantum communication will require to distribute quantum states over long distances.. The protocols implemented within such systems will include the distribution of high-dimensional and entangled quantum states. Indeed, spanning Hilbert spaces of greater dimensions allows higher information capacity and noise resilience, leading to enhanced quantum information processing [38, 85, 86]. In this context, VV states represent a powerful resource for classical and

quantum applications.

Here, we demonstrated the feasibility of distributing complex VV states through an OAM supporting fiber, also permitting to preserve entanglement with a different system. To fully assess the robustness to decoherence and quality of the transmitted complex entangled state, we performed quantum state tomographies, violations of CHSH-like inequalities and multipartite entanglement tests. The achieved fidelities of the transmitted state demonstrate the capability to perform high fidelity distribution in an OAM supporting fiber of a hybrid VV-polarization entangled state at the telecom wavelength. In particular, the possibility to simultaneously encode and distribute information in the polarization and OAM degree of freedom of a single particle represents an useful resource due to the higher robustness to losses, while tools for their processing have been identified [87]. This work paves the way towards adoption of high-dimensional entanglement in quantum networks. Further perspectives of this work involve the investigation of fiber-based distribution of different orders of OAM entangled states and their distribution over longer distances, exploiting the potential scalability arising from a fiber-based approach. Other perspectives involve interfacing of OAM integrated circuits [88–90] through OAM supporting fibers for future quantum networks.

Note added. During the preparation of this manuscript, the authors became aware of a work by Huan Cao *et al.* on a similar topic [91].

Funding Information

This work is supported by the Center of Excellence, SPOC - Silicon Photonics for Optical Communications (ref DNRF123), by the People Programme (Marie Curie Actions) of the European Union’s Seventh Framework Programme (FP7/2007-2013) under REA grant agreement n° 609405 (COFUNDPostdocDTU), and by the ERC-Advanced grant PHOSPhOR (Photonics of Spin-Orbit Optical Phenomena; Grant Agreement No. 694683). G.C acknowledges Becas Chile and Conicyt.

Acknowledgments

We thank S. Ramachandran and P. Gregg for the fiber design, P. Kristensen from OFS-Fitel for the fiber fabrication and D. Poderini for many advices on the software development.

References

- [1] N. Gisin and R. Thew, “Quantum communication,” *Nature Photonics*, vol. 1, no. 3, p. 165, 2007.
- [2] J.-W. Pan, D. Bouwmeester, H. Weinfurter, and A. Zeilinger, “Experimental entanglement swapping: entangling photons that never interacted,” *Physical Review Letters*, vol. 80, no. 18, p. 3891, 1998.
- [3] X.-S. Ma, S. Zotter, J. Kofler, R. Ursin, T. Jennewein, Č. Brukner, and A. Zeilinger, “Experimental delayed-choice entanglement swapping,” *Nature Physics*, vol. 8, no. 6, p. 479, 2012.
- [4] M. M. Weston, S. Slussarenko, H. M. Chrzanowski, S. Wollmann, L. K. Shalm, V. B. Verma, M. S. Allman, S. W. Nam, and G. J. Pryde, “Heralded quantum steering over a high-loss channel,” *Science Advances*, vol. 4, no. 1, p. e1701230, 2018.
- [5] Q.-C. Sun, Y.-L. Mao, Y.-F. Jiang, Q. Zhao, S.-J. Chen, W. Zhang, W.-J. Zhang, X. Jiang, T.-Y. Chen, L.-X. You, L. Li, Y.-D. Huang, X.-F. Chen, Z. Wang, X. Ma, Q. Zhang, and J.-W. Pan, “Entanglement swapping with independent sources over an optical-fiber network,” *Physical Review A*, vol. 95, no. 3, p. 032306, 2017.
- [6] J. T. Barreiro, T.-C. Wei, and P. G. Kwiat, “Beating the channel capacity limit for linear photonic superdense coding,” *Nature Physics*, vol. 4, no. 4, p. 282, 2008.
- [7] B. P. Williams, R. J. Sadler, and T. S. Humble, “Superdense coding over optical fiber links with complete bell-state measurements,” *Physical Review Letters*, vol. 118, no. 5, p. 050501, 2017.
- [8] C. Schuck, G. Huber, C. Kurtsiefer, and H. Weinfurter, “Complete deterministic linear optics bell state analysis,” *Physical Review Letters*, vol. 96, no. 19, p. 190501, 2006.
- [9] M. Barbieri, G. Vallone, P. Mataloni, and F. De Martini, “Complete and deterministic discrimination of polarization bell states assisted by momentum entanglement,” *Physical Review A*, vol. 75, no. 4, p. 042317, 2007.
- [10] D. Bouwmeester, J.-W. Pan, K. Mattle, M. Eibl, H. Weinfurter, and A. Zeilinger, “Experimental quantum teleportation,” *Nature*, vol. 390, p. 575, 1997.
- [11] D. Boschi, S. Branca, F. De Martini, L. Hardy, and S. Popescu, “Experimental realization of teleporting an unknown pure quantum state via dual classical and einstein-podolsky-rosen channels,” *Physical Review Letters*, vol. 80, p. 1121, 1998.
- [12] E. Lombardi, F. Sciarrino, S. Popescu, and F. De Martini, “Teleportation of a vacuum-one-photon qubit,” *Physical Review Letters*, vol. 88, p. 070402, 2002.

- [13] X.-L. Wang, X.-D. Cai, Z.-E. Su, M.-C. Chen, D. Wu, L. Li, N.-L. Liu, C.-Y. Lu, and J.-W. Pan, “Quantum teleportation of multiple degrees of freedom of a single photon,” *Nature*, vol. 518, no. 7540, p. 516, 2015.
- [14] I. Marcikic, H. De Riedmatten, W. Tittel, H. Zbinden, and N. Gisin, “Long-distance teleportation of qubits at telecommunication wavelengths,” *Nature*, vol. 421, no. 6922, p. 509, 2003.
- [15] L.-M. Duan, M. Lukin, J. I. Cirac, and P. Zoller, “Long-distance quantum communication with atomic ensembles and linear optics,” *Nature*, vol. 414, no. 6862, p. 413, 2001.
- [16] X.-S. Ma, T. Herbst, T. Scheidl, D. Wang, S. Kropatschek, W. Naylor, B. Wittmann, A. Mech, J. Kofler, E. Anisimova, V. Makarov, T. Jennewein, R. Ursin, and A. Zeilinger, “Quantum teleportation over 143 kilometres using active feed-forward,” *Nature*, vol. 489, no. 7415, p. 269, 2012.
- [17] A. Einstein, B. Podolsky, and N. Rosen, “Can quantum-mechanical description of physical reality be considered complete?,” *Physical Review*, vol. 47, no. 10, p. 777, 1935.
- [18] J. S. Bell, “On the Einstein Podolsky Rosen paradox,” *Physics Physique Fizika*, vol. 1, no. 3, p. 195, 1964.
- [19] R. Horodecki, P. Horodecki, M. Horodecki, and K. Horodecki, “Quantum entanglement,” *Reviews of Modern Physics*, vol. 81, no. 2, p. 865, 2009.
- [20] M. A. Nielsen and I. Chuang, *Quantum computation and quantum information*. AAPT, 2002.
- [21] N. Brunner, D. Cavalcanti, S. Pironio, V. Scarani, and S. Wehner, “Bell nonlocality,” *Reviews of Modern Physics*, vol. 86, no. 2, p. 419, 2014.
- [22] G. Adesso, T. R. Bromley, and M. Cianciaruso, “Measures and applications of quantum correlations,” *Journal of Physics A: Mathematical and Theoretical*, vol. 49, no. 47, p. 473001, 2016.
- [23] J. Yin, Y. Cao, Y.-H. Li, S.-K. Liao, L. Zhang, J.-G. Ren, W.-Q. Cai, W.-Y. Liu, B. Li, H. Dai, G.-B. Li, Q.-M. Lu, Y.-H. Gong, Y. Xu, S.-L. Li, F.-Z. Li, Y.-Y. Yin, Z.-Q. Jiang, M. Li, J.-J. Jia, G. Ren, D. He, Y.-L. Zhou, X.-X. Zhang, N. Wang, X. Chang, Z.-C. Zhu, N.-L. Liu, Y.-A. Chen, C.-Y. Lu, R. Shu, C.-Z. Peng, J.-Y. Wang, and J.-W. Pan, “Satellite-based entanglement distribution over 1200 kilometers,” *Science*, vol. 356, no. 6343, pp. 1140–1144, 2017.
- [24] R. Ursin, F. Tiefenbacher, T. Schmitt-Manderbach, H. Weier, T. Scheidl, M. Lindenthal, B. Blauensteiner, T. Jennewein, J. Perdigues, P. Trojek, Ömer B., M. Fürst, M. Meyenburg, J. Rarity, Z. Sodnik, C. Barbieri, H. Weinfurter, and A. Zeilinger, “Entanglement-based quantum communication over 144 km,” *Nature Physics*, vol. 3, no. 7, p. 629, 2007.
- [25] T. Honjo, S. W. Nam, H. Takesue, Q. Zhang, H. Kamada, Y. Nishida, O. Tadanaga, M. Asobe, B. Baek, R. Hadfield, S. Miki, M. Fujiwara, M. Sasaki, Z. Wang, and Y. Inoue, K. and. Yamamoto, “Long-distance entanglement-based quantum key distribution over optical fiber,” *Optics Express*, vol. 16, no. 23, pp. 19118–19126, 2008.
- [26] T. Inagaki, N. Matsuda, O. Tadanaga, M. Asobe, and H. Takesue, “Entanglement distribution over 300 km of fiber,” *Optics Express*, vol. 21, no. 20, pp. 23241–23249, 2013.
- [27] H. Hübel, M. R. Vanner, T. Lederer, B. Blauensteiner, T. Lorünser, A. Poppe, and A. Zeilinger, “High-fidelity transmission of polarization encoded qubits from an entangled source over 100 km of fiber,” *Optics Express*, vol. 15, no. 12, pp. 7853–7862, 2007.
- [28] A. Poppe, A. Fedrizzi, R. Ursin, H. Böhm, T. Lorünser, O. Maurhardt, M. Peev, M. Suda, C. Kurtsiefer, H. Weinfurter, T. Jennewein, and A. Zeilinger, “Practical quantum key distribution with polarization entangled photons,” *Optics Express*, vol. 12, no. 16, pp. 3865–3871, 2004.
- [29] F. Flamini, N. Spagnolo, and F. Sciarrino, “Photonic quantum information processing: a review,” *Reports on Progress in Physics*, vol. 82, p. 016001, 2019.
- [30] L. Allen, M. W. Beijersbergen, R. Spreeuw, and J. Woerdman, “Orbital angular momentum of light and the transformation of laguerre-gaussian laser modes,” *Physical Review A*, vol. 45, no. 11, p. 8185, 1992.
- [31] G. Molina-Terriza, J. P. Torres, and L. Torner, “Twisted photons,” *Nature Physics*, vol. 3, no. 5, p. 305, 2007.
- [32] N. Bozinovic, Y. Yue, Y. Ren, M. Tur, P. Kristensen, H. Huang, A. E. Willner, and S. Ramachandran, “Terabit-scale orbital angular momentum mode division multiplexing in fibers,” *Science*, vol. 340, no. 6140, pp. 1545–1548, 2013.
- [33] J. Wang, J.-Y. Yang, I. M. Fazal, N. Ahmed, Y. Yan, H. Huang, Y. Ren, Y. Yue, S. Dolinar, M. Tur, and A. E. Willner, “Terabit free-space data transmission employing orbital angular momentum multiplexing,” *Nature Photonics*, vol. 6, no. 7, p. 488, 2012.

- [34] A. E. Willner, H. Huang, Y. Yan, Y. Ren, N. Ahmed, G. Xie, C. Bao, L. Li, Y. Cao, Z. Zhao, J. Wang, M. P. J. Lavery, M. Tur, S. Ramachandran, A. F. Molisch, N. Ashrafi, and S. Ashrafi, “Optical communications using orbital angular momentum beams,” *Advances in Optics and Photonics*, vol. 7, no. 1, pp. 66–106, 2015.
- [35] K. Ingerslev, P. Gregg, M. Galili, F. Da Ros, H. Hu, F. Bao, M. A. U. Castaneda, P. Kristensen, A. Rubano, L. Marrucci, K. Rottwitt, T. Morioka, S. Ramachandran, and L. K. Oxenløwe, “12 mode, wdm, mimo-free orbital angular momentum transmission,” *Optics Express*, vol. 26, no. 16, pp. 20225–20232, 2018.
- [36] M. Malik, M. Erhard, M. Huber, M. Krenn, R. Fickler, and A. Zeilinger, “Multi-photon entanglement in high dimensions,” *Nature Photonics*, vol. 10, no. 4, p. 248, 2016.
- [37] J. Bavaresco, N. H. Valencia, C. Klöckl, M. Pivluska, P. Erker, N. Friis, M. Malik, and M. Huber, “Measurements in two bases are sufficient for certifying high-dimensional entanglement,” *Nature Physics*, vol. 14, no. 10, p. 1032, 2018.
- [38] M. Erhard, R. Fickler, M. Krenn, and A. Zeilinger, “Twisted photons: new quantum perspectives in high dimensions,” *Light: Science & Applications*, vol. 7, no. 3, p. 17146, 2018.
- [39] T. Giordani, E. Polino, S. Emiliani, A. Suprano, L. Innocenti, H. Majury, L. Marrucci, M. Paterostro, A. Ferraro, N. Spagnolo, and F. Sciarrino, “Experimental engineering of arbitrary qudit states with discrete-time quantum walks,” *Physical Review Letters*, vol. 122, no. 2, p. 020503, 2019.
- [40] A. C. Dada, J. Leach, G. S. Buller, M. J. Padgett, and E. Andersson, “Experimental high-dimensional two-photon entanglement and violations of generalized bell inequalities,” *Nature Physics*, vol. 7, no. 9, p. 677, 2011.
- [41] M. Krenn, R. Fickler, M. Fink, J. Handsteiner, M. Malik, T. Scheidl, R. Ursin, and A. Zeilinger, “Communication with spatially modulated light through turbulent air across vienna,” *New Journal of Physics*, vol. 16, no. 11, p. 113028, 2014.
- [42] F. Bouchard, A. Sit, F. Hufnagel, A. Abbas, Y. Zhang, K. Heshami, R. Fickler, C. Marquardt, G. Leuchs, W. R. Boyd, and E. Karimi, “Quantum cryptography with twisted photons through an outdoor underwater channel,” *Optics Express*, vol. 26, no. 17, pp. 22563–22573, 2018.
- [43] Y. Chen, W.-G. Shen, Z.-M. Li, C.-Q. Hu, Z.-Q. Yan, Z.-Q. Jiao, J. Gao, M.-M. Cao, K. Sun, and X.-M. Jin, “Underwater transmission of high-dimensional twisted photons over 55 meters,” *arXiv preprint arXiv:1902.01392*, 2019.
- [44] C. Brunet, P. Vaity, Y. Messaddeq, S. LaRochelle, and L. A. Rusch, “Design, fabrication and validation of an oam fiber supporting 36 states,” *Optics Express*, vol. 22, no. 21, pp. 26117–26127, 2014.
- [45] S. Li and J. Wang, “Supermode fiber for orbital angular momentum (oam) transmission,” *Optics Express*, vol. 23, no. 14, pp. 18736–18745, 2015.
- [46] B. Ndagano, R. Brüning, M. McLaren, M. Duparré, and A. Forbes, “Fiber propagation of vector modes,” *Optics Express*, vol. 23, no. 13, pp. 17330–17336, 2015.
- [47] D. Cozzolino, D. Bacco, B. Da Lio, K. Ingerslev, Y. Ding, K. Delgaard, P. Kristensen, M. Galili, K. Rottwitt, S. Ramachandran, and L. K. Oxenløwe, “Fiber based high-dimensional quantum communication with twisted photons,” *arXiv preprint arXiv:1803.10138*, 2018.
- [48] A. Sit, R. Fickler, F. Alsaïari, F. Bouchard, H. Larocque, P. Gregg, L. Yan, R. W. Boyd, S. Ramachandran, and E. Karimi, “Quantum cryptography with structured photons through a vortex fiber,” *Optics Letters*, vol. 43, no. 17, pp. 4108–4111, 2018.
- [49] P. Gregg, P. Kristensen, and S. Ramachandran, “Conservation of orbital angular momentum in air-core optical fibers,” *Optica*, vol. 2, no. 3, pp. 267–270, 2015.
- [50] M. R. Dennis, K. O’Holleran, and M. J. Padgett, “Singular optics: Optical vortices and polarization singularities,” vol. 53 of *Progress in Optics*, pp. 293–363, Elsevier, 2009.
- [51] Q. Zhan, “Cylindrical vector beams: from mathematical concepts to applications,” *Advances in Optics and Photonics*, vol. 1, no. 1, pp. 1–57, 2009.
- [52] F. Cardano, E. Karimi, S. Slussarenko, L. Marrucci, C. de Lisio, and E. Santamato, “Polarization pattern of vector vortex beams generated by q-plates with different topological charges,” *Applied Optics*, vol. 51, no. 10, pp. C1–C6, 2012.
- [53] G. Milione, H. I. Sztul, D. A. Nolan, and R. R. Alfano, “Higher-order Poincaré sphere, stokes parameters, and the angular momentum of light,” *Physical Review Letters*, vol. 107, p. 053601, 2011.
- [54] A. F. Abouraddy and K. C. Toussaint Jr, “Three-dimensional polarization control in microscopy,” *Physical Review Letters*, vol. 96, no. 15, p. 153901, 2006.

- [55] B. J. Roxworthy and K. C. Toussaint Jr, “Optical trapping with π -phase cylindrical vector beams,” *New Journal of Physics*, vol. 12, no. 7, p. 073012, 2010.
- [56] H. Moradi, V. Shahabadi, E. Madadi, E. Karimi, and F. Hajizadeh, “Efficient optical trapping with cylindrical vector beams,” *Optics Express*, vol. 27, p. 7266, 2019.
- [57] V. D’Ambrosio, N. Spagnolo, L. Del Re, S. Slussarenko, Y. Li, L. C. Kwek, L. Marrucci, S. P. Walborn, L. Aolita, and F. Sciarrino, “Photonic polarization gears for ultra-sensitive angular measurements,” *Nature Communications*, vol. 4, p. 2432, 2013.
- [58] F. K. Fatemi, “Cylindrical vector beams for rapid polarization-dependent measurements in atomic systems,” *Optics Express*, vol. 19, no. 25, pp. 25143–25150, 2011.
- [59] A. Büse, M. L. Juan, N. Tischler, V. D’Ambrosio, F. Sciarrino, L. Marrucci, and G. Molina-Terriza, “Symmetry protection of photonic entanglement in the interaction with a single nanoaperture,” *Physical Review Letters*, vol. 121, p. 173901, 2018.
- [60] V. Parigi, V. D’Ambrosio, C. Arnold, L. Marrucci, F. Sciarrino, and J. Laurat, “Storage and retrieval of vector beams of light in a multiple-degree-of-freedom quantum memory,” *Nature Communications*, vol. 6, p. 7706, 2015.
- [61] V. D’Ambrosio, G. Carvacho, F. Graffitti, C. Vitelli, B. Piccirillo, L. Marrucci, and F. Sciarrino, “Entangled vector vortex beams,” *Physical Review A*, vol. 94, no. 3, p. 030304, 2016.
- [62] B. Ndagano, I. Nape, M. A. Cox, C. Rosales-Guzman, and A. Forbes, “Creation and detection of vector vortex modes for classical and quantum communication,” *Journal of Lightwave Technology*, vol. 36, no. 2, pp. 292–301, 2018.
- [63] Y. S. Rumala, G. Milione, T. A. Nguyen, S. Pratavieira, Z. Hossain, D. Nolan, S. Slussarenko, E. Karimi, L. Marrucci, and R. R. Alfano, “Tunable supercontinuum light vector vortex beam generator using a q-plate,” *Optics Letters*, vol. 38, no. 23, pp. 5083–5086, 2013.
- [64] V. D’Ambrosio, E. Nagali, S. P. Walborn, L. Aolita, S. Slussarenko, L. Marrucci, and F. Sciarrino, “Complete experimental toolbox for alignment-free quantum communication,” *Nature Communication*, vol. 3, p. 961, 2012.
- [65] G. Vallone, V. D’Ambrosio, A. Sponselli, S. Slussarenko, L. Marrucci, F. Sciarrino, and P. Villoresi, “Free-space quantum key distribution by rotation-invariant twisted photons,” *Physical Review Letters*, vol. 113, p. 060503, 2014.
- [66] G. Carvacho, F. Graffitti, V. D’Ambrosio, and F. Hiesmayr, B. Sciarrino, “Experimental investigation on the geometry of GHZ states,” *Scientific Reports*, vol. 7, p. 13265, 2017.
- [67] F. Bouchard, K. Heshami, D. England, R. Fickler, R. W. Boyd, B.-G. Englert, L. Sánchez-Soto, and E. Karimi, “Experimental investigation of high-dimensional quantum key distribution protocols with twisted photons,” *Quantum*, vol. 2, p. 111, 2018.
- [68] L. Marrucci, C. Manzo, and D. Paparo, “Optical spin-to-orbital angular momentum conversion in inhomogeneous anisotropic media,” *Physical Review Letters*, vol. 96, no. 16, p. 163905, 2006.
- [69] L. Marrucci, E. Karimi, S. Slussarenko, B. Piccirillo, E. Santamato, E. Nagali, and F. Sciarrino, “Spin-to-orbital conversion of the angular momentum of light and its classical and quantum applications,” *Journal of Optics*, vol. 13, no. 6, p. 064001, 2011.
- [70] E. Nagali, F. Sciarrino, F. De Martini, L. Marrucci, B. Piccirillo, E. Karimi, and E. Santamato, “Quantum information transfer from spin to orbital angular momentum of photons,” *Physical Review Letters*, vol. 103, no. 1, p. 013601, 2009.
- [71] D. F. James, P. G. Kwiat, W. J. Munro, and A. G. White, “On the measurement of qubits,” in *Asymptotic Theory Of Quantum Statistical Inference: Selected Papers*, pp. 509–538, World Scientific, 2005.
- [72] J. F. Clauser, M. A. Horne, A. Shimony, and R. A. Holt, “Proposed experiment to test local hidden-variable theories,” *Physical Review Letters*, vol. 23, no. 15, p. 880, 1969.
- [73] N. D. Mermin, “Extreme quantum entanglement in a superposition of macroscopically distinct states,” *Physical Review Letters*, vol. 65, no. 15, p. 1838, 1990.
- [74] M. Ardehali, “Bell inequalities with a magnitude of violation that grows exponentially with the number of particles,” *Physical Review A*, vol. 46, no. 9, p. 5375, 1992.
- [75] A. Belinskii and D. N. Klyshko, “Interference of light and bell’s theorem,” *Physics-Uspekhi*, vol. 36, no. 8, p. 653, 1993.
- [76] L. Hardy, “Quantum mechanics, local realistic theories, and Lorentz-invariant realistic theories,” *Physical Review Letters*, vol. 68, no. 20, p. 2981, 1992.
- [77] L. Hardy, “Nonlocality for two particles without inequalities for almost all entangled states,” *Physical Review Letters*, vol. 71, no. 11, p. 1665, 1993.

- [78] S.-H. Jiang, Z.-P. Xu, H.-Y. Su, A. K. Pati, and J.-L. Chen, “Generalized Hardy’s paradox,” *Physical Review Letters*, vol. 120, no. 5, p. 050403, 2018.
- [79] S. Kochen and E. P. Specker, “The problem of hidden variables in quantum mechanics,” in *The logico-algebraic approach to quantum mechanics*, pp. 293–328, Springer, 1975.
- [80] E. Karimi, J. Leach, S. Slussarenko, B. Piccirillo, L. Marrucci, L. Chen, W. She, S. Franke-Arnold, M. J. Padgett, and E. Santamato, “Spin-orbit hybrid entanglement of photons and quantum contextuality,” *Physical Review A*, vol. 82, no. 2, p. 022115, 2010.
- [81] A. Aiello, F. Töppel, C. Marquardt, E. Giacobino, and G. Leuchs, “Quantum-like nonseparable structures in optical beams,” *New Journal of Physics*, vol. 17, no. 4, p. 043024, 2015.
- [82] M. McLaren, T. Konrad, and A. Forbes, “Measuring the nonseparability of vector vortex beams,” *Physical Review A*, vol. 92, no. 2, p. 023833, 2015.
- [83] D. Collins, N. Gisin, S. Popescu, D. Roberts, and V. Scarani, “Bell-type inequalities to detect true n-body nonseparability,” *Physical Review Letters*, vol. 88, no. 17, p. 170405, 2002.
- [84] J.-D. Bancal, N. Gisin, Y.-C. Liang, and S. Pironio, “Device-independent witnesses of genuine multipartite entanglement,” *Physical Review Letters*, vol. 106, no. 25, p. 250404, 2011.
- [85] H. Bechmann-Pasquinucci and W. Tittel, “Quantum cryptography using larger alphabets,” *Physical Review A*, vol. 61, no. 6, p. 062308, 2000.
- [86] N. J. Cerf, M. Bourennane, A. Karlsson, and N. Gisin, “Security of quantum key distribution using d-level systems,” *Physical Review Letters*, vol. 88, no. 12, p. 127902, 2002.
- [87] C. Vitelli, N. Spagnolo, L. Aparo, F. Sciarrino, E. Santamato, and L. Marrucci, “Joining the quantum state of two photons into one,” *Nature Photonics*, vol. 7, no. 7, p. 521, 2013.
- [88] X. Cai, J. Wang, M. J. Strain, B. Johnson-Morris, J. Zhu, M. Sorel, J. L. O’Brien, M. G. Thompson, and S. Yu, “Integrated compact optical vortex beam emitters,” *Science*, vol. 338, no. 6105, pp. 363–366, 2012.
- [89] Y. Chen, J. Gao, Z.-Q. Jiao, K. Sun, W.-G. Shen, L.-F. Qiao, H. Tang, X.-F. Lin, and X.-M. Jin, “Mapping twisted light into and out of a photonic chip,” *Physical Review Letters*, vol. 121, no. 23, p. 233602, 2018.
- [90] J. Liu, S.-M. Li, L. Zhu, A.-D. Wang, S. Chen, C. Klitis, C. Du, Q. Mo, M. Sorel, S.-Y. Yu, X.-L. Cai, and J. Wang, “Direct fiber vector eigenmode multiplexing transmission seeded by integrated optical vortex emitters,” *Light: Science & Applications*, vol. 7, no. 3, p. 17148, 2018.
- [91] H. Cao, S.-C. Gao, C. Zhang, J. Wang, D.-Y. He, B.-H. Liu, Z.-W. Zhou, G.-X. Zhu, Y.-J. Chen, Z.-H. Li, S.-Y. Yu, H. Yun-Feng, C.-F. Li, and G.-C. Guo, “Distribution of high-dimensional orbital angular momentum entanglement at telecom wavelength over 1km oam fiber,” *arXiv preprint arXiv:1811.12195*, 2018.